A&A 443, L7–L10 (2005)
DOI: 10.1051/0004-6361:200500179

Astronomy & Astrophysics

Multi-line spectroscopy of dark-cored penumbral filaments

L. R. Bellot Rubio[1], K. Langhans[2], and R. Schlichenmaier[3]

[1] Instituto de Astrofísica de Andalucía (CSIC), Apdo 3004, 18080 Granada, Spain
e-mail: lbellot@iaa.es
[2] Institute for Solar Physics, Royal Swedish Academy of Sciences, Alba Nova University Center, 10691 Stockholm, Sweden
[3] Kiepenheuer-Institut für Sonnenphysik, Schöneckstr. 6, 79104 Freiburg, Germany

Received 1 July 2005 / Accepted 3 September 2005

ABSTRACT

Dark-cored filaments could be the basic building blocks of sunspot penumbrae. Yet, their nature and physical conditions are unknown. In an attempt to improve this situation, we present the first high-resolution spectra of dark-cored penumbral filaments. Several such filaments were observed near the umbra/penumbra boundary of a sunspot located at heliocentric angles of 5° and 20°. Our data reveal (a) significantly larger Doppler shifts in the dark cores as compared to their lateral brightenings; (b) Doppler shifts that increase with depth in the photosphere, up to 1.5 km s^{-1}; and (c) Doppler shifts that increase with increasing heliocentric distance. The Doppler velocities measured in the dark cores are almost certainly produced by upflows. In addition, dark-cored penumbral filaments exhibit weaker fields than their surroundings (by 100−300 G). These results provide new constraints for models of dark-cored penumbral filaments.

Key words. Sunspots – Sun: photosphere – line: profiles

1. Introduction

Recent imaging observations with the Swedish 1-m Solar Telescope (SST) have demonstrated that many penumbral filaments possess internal structure in the form of a dark core (Scharmer et al. 2002; Rouppe van der Voort et al. 2004). The dark core is surrounded by two narrow lateral brightenings, both of which move with the same speed and direction as a single entity. The existence of dark-cored filaments has been confirmed by Sütterlin et al. (2004). The common occurrence of dark-cored filaments and the fact that their various parts show a coherent behavior have raised expectations that they could be the fundamental constituents of the penumbra. The origin of these structures, however, remains enigmatic.

Our understanding of dark-cored filaments has been limited by a significant lack of knowledge of their magnetic and kinematic properties. The observational characterization of these structures is a difficult endeavor due to the very small spatial scales involved. Recently, Langhans et al. (2005) have presented 0.″2-resolution longitudinal magnetograms of dark-cored filaments in the blue wing of the Fe I 630.25 nm line. The circular polarization signal in the dark cores was found to be significantly lower than in the lateral edges, suggesting weaker and/or more inclined fields. Unfortunately, these data do not allow to discriminate between the two possibilities. The flow field in dark-cored filaments is largely unknown.

The purpose of this Letter is to shed light on some essential questions concerning dark-cored filaments: are the dark cores associated with Doppler shifts (i.e., do they carry Evershed flows)? Is the field strength different in the dark-cored filaments and their surroundings? We investigate these issues by examining high-resolution spectroscopic observations of a sunspot penumbra in three photospheric lines.

2. Observations, data reduction, and data analysis

We have used the TRIPPEL spectrograph (Kiselman et al. 2005) and the adaptive optics system of the SST on La Palma (Spain) to observe the main spot of NOAA AR 10756 on three different days: April 29, 2005 (θ = 19.5°); May 1, 2005 (θ = 5°); and May 2, 2005 (θ = 20.5°). With a slit width of 25 μm (0.″11), the nominal resolving power of the spectrograph is around 240 000. Simultaneous spectra of the Fe I 557.6 nm, Fe II 614.9 nm, and Fe I 709.0 nm lines were recorded on three Kodak Megaplus 1.6i cameras (see Table 1 for details). Two additional cameras were used to take simultaneous slit-jaw images through 1-nm wide filters centered at 532 nm and 694 nm. Their exposure times were adjusted to match those of the spectral cameras. Finally, the spot was imaged through a G-band continuum filter (436.4 nm) with exposure times of ~20 ms in order to obtain movies and context information.

We performed short (<20″) scans of AR 10756 with a step size of 0.″1. Due to the enhanced visibility of dark-cored filaments in the center-side penumbra, most of our scans were carried out in this part of the spot. A few scans of the limb-side penumbra were performed on May 2, 2005. The spectral images have been corrected for dark current, gain table variations, and deformations introduced by the spectrograph.

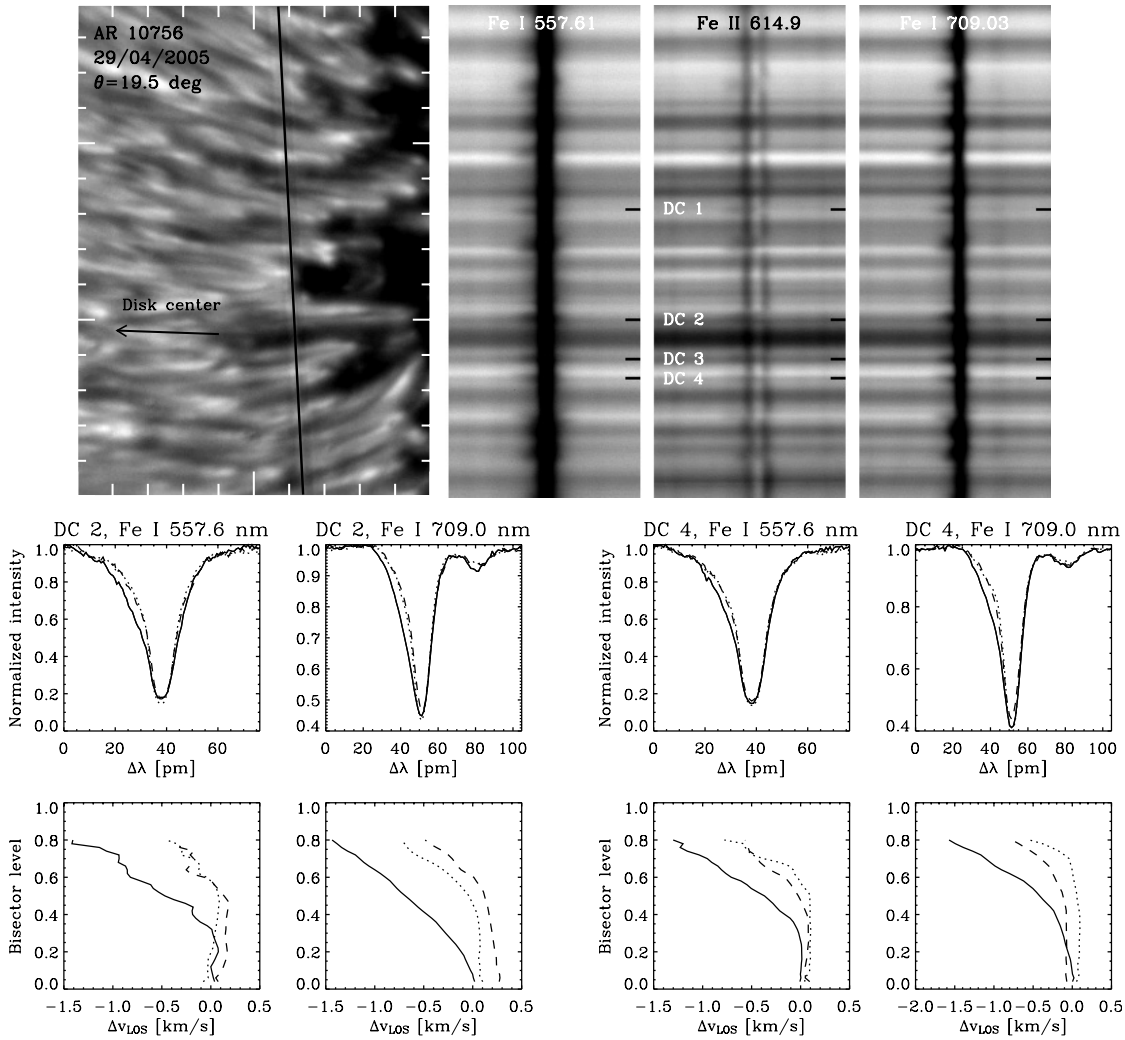

Fig. 1. *Top*: slit-jaw image of AR 10756 on April 29 (λ = 532 nm) and simultaneous spectral images showing the Fe I 557.6 nm, Fe II 614.9 nm, and Fe I 709.0 nm lines along the slit. Tick marks are arcsec. Four dark-cored filaments are crossed by the slit; they are numbered 1–4 from top to bottom. The dark cores are marked with small horizontal dashes in the spectral images. *Middle*: normalized Fe I 557.6 nm and Fe I 709.0 nm intensity profiles emerging from dark cores 2 and 4 (solid lines), and their lateral brightenings (±0.″2 on either side; dotted and dashed lines). *Bottom*: bisectors observed in the dark cores (solid lines) and the lateral edges (dotted and dashed lines). Negative velocities indicate blueshifts.

Table 1. Details of the spectral cameras used.

Spectral region	Dispersion [pm px^{-1}]	Exposure time [ms]	Pixel size [″]
557.6 nm	0.763	280–350	0.04
614.9 nm	0.887	220–300	0.04
709.0 nm	1.046	160–200	0.04

In this study we consider only spectra taken during excellent seeing conditions. Even with relatively large exposure times, we have 7 examples of dark-cored filaments with clearly visible intensity dips in both the slit-jaw and spectral images (see Fig. 1). From the intensity cuts presented in Fig. 3, we estimate a spatial resolution of ∼0.″2 in the best spectral images.

The flow field in dark-cored penumbral filaments is investigated through a bisector analysis of the non-magnetic Fe I 557.6 nm and Fe I 709.0 nm lines. Bisectors are computed for intensity levels from 4% to 80%, with 0% representing the line core and 100% the continuum. Whenever possible, an absolute velocity calibration has been performed. For the 709.0 nm region, we have used the telluric H_2O line at 709.4050 nm as a fixed reference. Its wavelength has been determined from the FTS atlas of Brault & Neckel (1987). The velocities obtained from the bisector shifts of Fe I 709.0 nm are corrected for gravitational redshift, orbital motion, Earth rotation, and solar rotation as explained by Martínez Pillet et al. (1997). The precision of our absolute velocity calibration is on the order of 100 m s^{-1}. The telluric line is too weak on April 29 and May 2, so the absolute calibration of Fe I 709.0 nm has been performed only for May 1. The 557.6 nm spectral region does not contain any suitable telluric line. When no absolute calibration is available, we set the zero point of the velocity scale at the line core position of the profile emerging from the dark core. We believe that such a relative calibration provides velocities which do not differ by more than a few hundred m s^{-1} from the real ones. This is certainly the case for Fe I 709.0 nm on May 1. It should also be the case for Fe I 557.6 nm: the

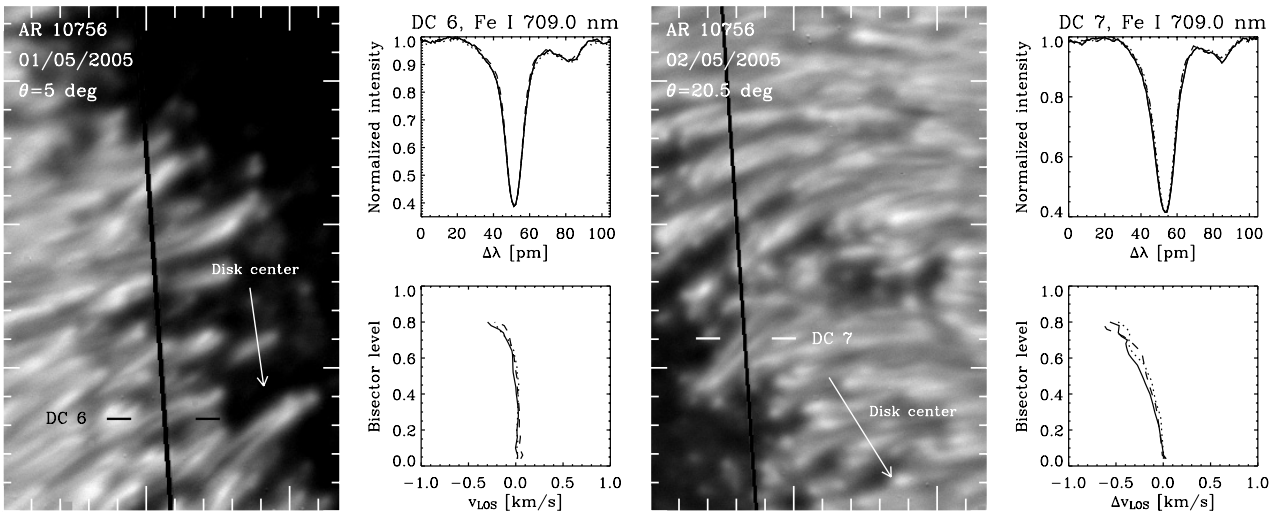

Fig. 2. *Left*: slit-jaw image of AR 10756 on May 1 (λ = 694 nm), normalized Fe I 709.0 nm profiles, and bisectors. *Right*: same, for May 2.

high-resolution (0.″5) spectra analyzed by Schlichenmaier et al. (2004) indicate line-core velocities smaller than 200 m s^{-1} everywhere in the penumbra.

The field strength of dark-cored penumbral filaments is estimated from the nearly complete magnetic splitting of the Fe II 614.9 nm line ($g_{\rm eff}$ = 4/3). This line is particularly suited for such measurements because it does not possess a central π component (Lites 1993). In the strong field regime, the wavelength separation of the Zeeman components depends only on the field strength, not on the field inclination. We restrict our analysis to those profiles with little differences between the Zeeman components: sometimes, the observed profiles are rather asymmetric, perhaps due to velocity gradients and/or molecular blends. Our estimates of the field strength are sensitive to noise, and therefore we use them only to reveal general trends. The accuracy in the derived values is not better than 50−100 G.

3. Results

3.1. Doppler shifts

The upper panels of Fig. 1 show slit-jaw and spectral images of the inner center-side penumbra on April 29 (θ = 19.5°). The slit crosses four well defined dark-cored filaments. The dark cores are easy to identify in the spectral images of Fe I 557.6 nm and Fe I 709.0 nm, as they display large "spikes" to the blue. Other dark structures along the slit also show blueshifts, but not that prominent or localized. Interestingly, the lateral brightenings do not exhibit significant spikes.

The spectral images make it clear that dark cores are associated with Doppler shifts. To investigate their properties in more detail, the lower panels of Fig. 1 display normalized profiles and bisectors at the position of two filaments. While the red wings of the profiles from the dark cores and the lateral brightenings are very similar, the blue wing is strongly blueshifted in the former. As a result, the bisectors of the dark cores show large tilts, with blueshifts of 1.5 km s^{-1} near the continuum and negligible shifts close to line center. The lateral edges, at a distance of ±0.″2 from the dark cores, exhibit much smaller blueshifts (a few hundred m s^{-1}), and only near the continuum. We note, however, that the bisector shapes change smoothly across the filaments: closer to the dark cores, the lateral brightenings show larger blueshifts.

The left part of Fig. 2 displays a slit-jaw image, line profiles and bisectors of the center-side penumbra on May 1 (θ = 5°). In this case the slit crosses two dark-cored filaments; we only discuss the profiles of one of them, and only for Fe I 709.0 nm, as the other filament and Fe I 557.6 nm indicate a similar behavior. At an heliocentric distance of 5°, the bisectors of the dark cores and the lateral brightenings exhibit very small blueshifts, with maximum values of 0.3 km s^{-1} at intensity levels of 80%. The spectral spikes observed at θ = 19.5° have disappeared completely as a result of the geometry, which is less favorable for the detection of nearly horizontal flows.

Finally, the right part of Fig. 2 displays a dark-cored filament in the limb-side penumbra of AR 10756 on May 2, when the spot was 20.5° off the disk center. The angle between this filament and the direction to the limb is 78°, i.e., the horizontal velocity component of a radial outflow in the filament would produce a redshift. Yet, as for the center-side filaments of April 29, we observe blueshifts with maximum values of 0.5 km s^{-1} near the continuum. Since the proper motion of the filament (determined from a movie of G-band continuum images) produces a blueshift of only 20 m s^{-1}, the observed blueshifts must be interpreted as being due to upflows.

3.2. Field strengths

Figure 3 shows the continuum intensity and field strength across four dark-cored filaments observed on April 29 and May 1. These examples demonstrate that the field strength is weaker in the dark-cored filaments as compared to their surroundings. The difference amounts to up to 300 G, i.e., it is well above the uncertainty of our estimates. We also note the tendency for the dark cores to have weaker fields than their lateral edges. Since the difference is only about 100 G, and not always seen, additional observations are needed to confirm this result.

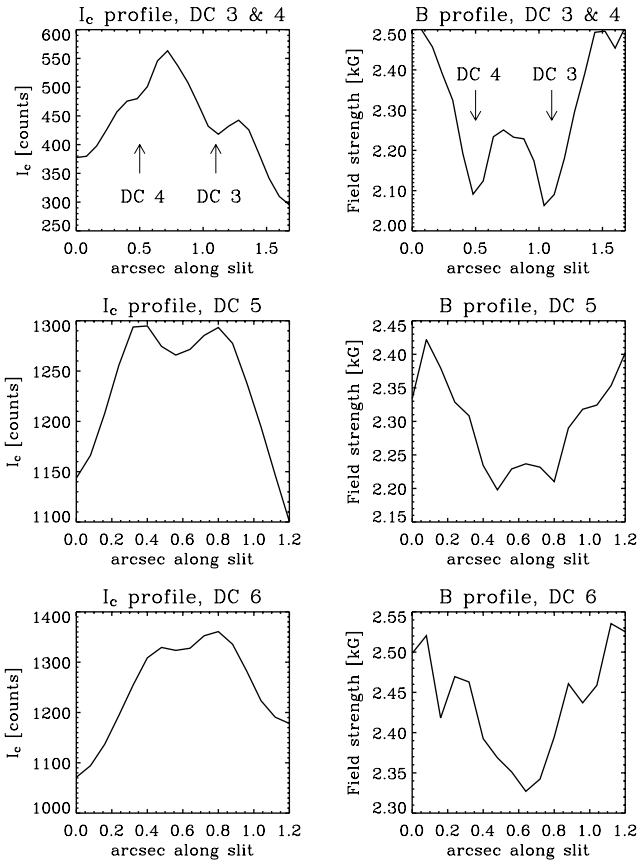

Fig. 3. Continuum intensity at 614.9 nm (*left*) and field strength (*right*) across four dark-cored filaments observed on April 29 and May 1. To minimize the effect of noise, the field strength curves have been computed from Fe II 614.9 nm profiles averaged over three pixels (0.″12).

4. Discussion

At a spatial resolution of 0.″2, the non-magnetic Fe I 557.6 nm and Fe I 709.0 nm lines emerging from seven dark-cored filaments close to the umbra/penumbra boundary reveal blueshifts associated with the dark cores and their lateral brightenings. Blueshifts are found in both center and limb-side filaments at heliocentric angles of 5° and 20°. The maximum blueshifts occur in the line wing near the continuum, which is highly suggestive of deep-lying flows (cf. Schlichenmaier et al. 2004).

The LOS projection of a flow of magnitude v and inclination γ with respect to the local vertical is given by

$$v_{\rm LOS} = -v\,(\cos\gamma\cos\theta - \sin\gamma\cos\varphi\sin\theta), \quad (1)$$

where φ stands for the angle between the filament and the line of symmetry (φ is 0° and 180° for filaments parallel to the line of symmetry on the limb side and the center side, respectively). The fact that we do not observe redshifts in the dark-cored filaments of May 1 ($\theta = 5°$, $\varphi = 109°$) sets strong limits on the maximum inclination of the flow: in order to produce blueshifts, the Evershed flow could not have had an inclination to the local vertical larger than 92°, otherwise the line profiles would have been shifted to the red. But the strongest constraint on the flow inclination comes from our limb-side dark-cored filament of May 2, observed at $\theta = 20.5°$ and $\varphi = 78°$. For the flow to produce a blueshift in this part of the inner penumbra, its inclination had to be smaller than 85°.

These results indicate that the Evershed flow at the umbra/penumbra boundary is almost certainly an *upflow* with large horizontal velocities and no downflowing component. The flow inclination may vary with distance from the inner footpoint, but our data do not permit us to confirm this hypothesis. Also, the flow seems to be more intense in the dark cores than in the lateral brightenings, at least for the April 29 filaments.

In summary, we find that the Evershed flow is concentrated in the dark cores, that it has an upflow component, and that dark-cored filaments possess weaker magnetic fields than their surroundings. These results are compatible with the idea of an uncombed penumbra (Solanki & Montavon 1993); indeed, almost all spectropolarimetric analyses published to date (e.g., Lites et al. 1993; Bellot Rubio et al. 2004; Borrero et al. 2005) agree that the Evershed flow occurs preferentially in the weaker and more horizontal magnetic fields (which are inclined upward in the inner penumbra). Our results are also in qualitative agreement with simulations of moving magnetic flux tubes as being the cause of flow filaments (Schlichenmaier 2002). Hence, in the context of the uncombed model and the moving tube model, a dark-cored filament would be the manifestation of a penumbral flux tube, although it is unclear at present how the dark cores are formed. Finding the mechanism responsible for the dark cores is the challenge; hopefully, the constraints set by our analysis will facilitate the search.

Acknowledgements. This work has been supported by the Spanish MCyT under *Programa Ramón y Cajal* and project ESP2003-07735-C04-03, and by the German DFG under grant SCHL 514/2–1. KL's research is funded by the European Community through the European Solar Magnetism Network (contract HPRN-CT-2002-00313). The SST is operated by the Royal Swedish Academy of Sciences in the Spanish Observatorio del Roque de los Muchachos of the IAC.

References

Bellot Rubio, L. R., Balthasar, H., & Collados, M. 2004, A&A, 427, 319
Borrero, J. M., Lagg, A., Solanki, S. K., & Collados, M. 2005, A&A, 436, 333
Brault, J., & Neckel, H. 1987, Spectral Atlas of Solar Disk-Averaged and Disk-Center Intensity from 3290 to 12 510 Å
Kiselman, D., et al. 2005, A&A, in preparation
Langhans, K., Scharmer, G. B., Kiselman, D., Löfdahl, M. G., & Berger, T. E. 2005, A&A, 436, 1087
Lites, B. W. 1993, Sol. Phys., 143, 229
Lites, B. W., Elmore, D. F., Seagraves, P., & Skumanich, A. P. 1993, ApJ, 418, 928
Martínez Pillet, V., Lites, B. W., & Skumanich, A. 1997, ApJ, 474, 810
Rouppe van der Voort, L. H. M., Löfdahl, M. G., Kiselman, D., & Scharmer, G. B. 2004, A&A, 414, 717
Scharmer, G. B., Gudiksen, B. V., Kiselman, D., Löfdahl, M. G., & Rouppe van der Voort, L. H. M. 2002, Nature, 420, 151
Schlichenmaier, R. 2002, AN, 323, 303
Schlichenmaier, R., Bellot Rubio, L. R., & Tritschler, A. 2004, A&A, 415, 731
Solanki, S. K., & Montavon, C. A. P. 1993, A&A, 275, 283
Sütterlin, P., Bellot Rubio, L. R., & Schlichenmaier, R. 2004, A&A, 424, 1049